From electrostatics to electrochemistry
rethinking volta potential in nowadays and future in-situ kelvin probe studies

Rahimi, Ehsan; Mesquida, Patrick; Glatzel, Thilo; Garcia, Yaiza Gonzalez; Mol, Arjan

DOI
10.1016/j.electacta.2025.147702

Publication date
2026

Document Version
Final published version

Published in
Electrochimica Acta

Electrochimica Acta 545 (2026) 147702

Contents lists available at ScienceDirect

Electrochimica Acta

journal homepage: www.journals.elsevier.com/electrochimica-acta

From electrostatics to electrochemistry: rethinking volta potential in nowadays and future in-situ kelvin probe studies

Ehsan Rahimi [a,*], Patrick Mesquida [b], Thilo Glatzel [c], Yaiza Gonzalez Garcia [a], Arjan Mol [a]

[a] Department of Materials Science and Engineering, Delft University of Technology, Mekelweg 2, 2628 CD, Delft, Netherlands
[b] Department of Physics, King's College London, Strand, London WC2R 2LS, UK
[c] Department of Physics, University of Basel, Klingelbergstrasse 82, 4056 Basel, Switzerland

ARTICLE INFO

Keywords:
Kelvin probe
Volta potential
AC-KPFM
OL-EPM
Electrochemistry
Corrosion
Degradation

ABSTRACT

The Volta potential (also known as contact potential) is widely used in Kelvin probe studies of corrosion, energy materials, and biomaterials, but its relation to electrochemical behavior in solution, and its possible interpretation as an electrochemical signal, remains debated and is often inconsistent. Here, we clarify the conditions under which the electrostatic contrast revealed by Kelvin probe measurements can be meaningfully correlated with redox-related behavior, and when such interpretation is not valid. We also argue for terminology that is consistent with physical theory, interfacial chemistry, and recent methodological advances such as alternating current Kelvin probe force microscopy (AC-KPFM) and open-loop electric potential microscopy (OL-EPM).

1. Critical appraisal of kelvin probe studies across a wide variety of application domains

Kelvin probe techniques are non-contact, non-destructive methods that measure the contact potential difference (CPD) or electrostatic surface potential difference (ESPD), the DC voltage resulting from differences in vacuum work function between a conductive probe and the sample surface [1–3]. The CPD reflects surface electrostatics and is influenced by phenomena such as band bending, surface dipoles, and localized charge distributions [4–6]. Measurements are typically carried out under controlled environments such as vacuum, dry or relatively humid atmospheric conditions, or even with thin film electrolytes, depending on the specific application [7,8].

Within this framework, two principal modalities are employed to probe the ESPD. The macroscopic scanning Kelvin probe (SKP) employs a vibrating reference probe positioned above the surface to form a capacitor, typically covering millimeter- to micrometer-scale areas [9, 10]. In contrast, the scanning Kelvin probe force microscopy (SKPFM or KPFM) technique integrates the same fundamental principle of the Kelvin probe into an atomic force microscopy (AFM) platform, a configuration first introduced by Weaver [11] and then extended by Nonnenmacher [12]. In KPFM, it is the AFM cantilever itself that oscillates, allowing the system to maintain nanometer-scale spatial resolution. This same oscillation (e.g., the cantilever still oscillates at the same resonance frequency) is used for topography imaging in the first pass of a given scan line and for detecting electrostatic forces in the second pass at some height above that same scan line. KPFM is a versatile nanoscale technique that is widely used across disciplines such as semiconductor devices, nanostructures, energy materials, and biomaterials to map ESPD, influenced charge distribution, and work function differences [4,13–15]. It provides essential insights into the electronic structure, defects, interfaces, and surface reactions of both functional and structural materials at micro, nano, and atomic scales [16,17].

Nevertheless, in corrosion science, SKP is widely employed to investigate the atmospheric corrosion of metallic surfaces and the underfilm delamination of coated substrates in controlled high-humidity or thin-film electrolyte conditions [18–20]. For coated substrates, once the

Abbreviation: AC, Alternating current; AC-KPFM, Alternating current Kelvin probe force microscopy; AFM, Atomic force microscopy; CPD, Contact potential difference; DC, Direct current; DC-KPFM, Direct current Kelvin probe force microscopy; EDL, Electric double layer; EDXS, Energy dispersive X-ray spectroscopy; E_{corr}, Corrosion potential; ESPD, Electrostatic surface potential difference; GB, Grain boundaries; KPFM, Kelvin probe force microscopy; OL-EPM, Open-loop electric potential microscopy; RH, Relative humidity; SECM, Scanning electrochemical microscopy; SEM, Scanning electron microscopy; SKP, Scanning Kelvin probe; SKPFM, Scanning Kelvin probe force microscopy; $\tilde{\mu}$, Electrochemical potential.

* Corresponding author.
E-mail address: e.rahimi-2@tudelft.nl (E. Rahimi).

https://doi.org/10.1016/j.electacta.2025.147702
Received 3 September 2025; Received in revised form 8 October 2025; Accepted 1 November 2025
Available online 2 November 2025

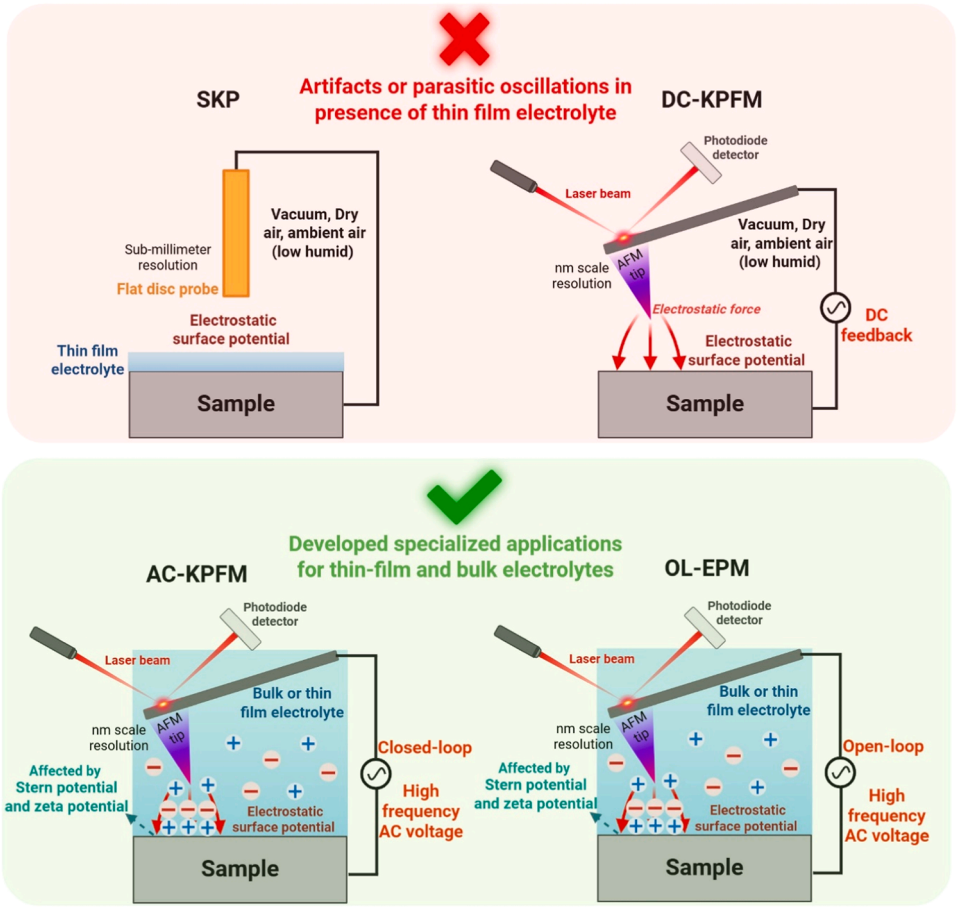

Fig. 1. Comparative schematic of SKP, DC-KPFM, AC-KPFM, and OL-EPM techniques, showing their operational scale, spatial resolution, environmental compatibility, and interpretation of measured ESPD.

relative humidity exceeds a critical threshold, tens of nano to micrometer-thick electrolyte films develop at the coating–metal interface due to water diffusion or defects. In such circumstances, the measured CPD may approximate local electrochemical tendencies, such as corrosion potential (E_{corr}) contrasts between galvanically coupled phases [21,22]. This is the context in which the term "Volta potential" became widely adopted, often interpreted as a spatially resolved electrochemical indicator [8,9]. While this interpretation can be meaningful under specific environmental conditions, it must be applied with care, as the signal remains fundamentally electrostatic in origin and highly sensitive to surface physicochemical conditions (native oxide film, roughness, contamination during cleaning process, etc.), electrolyte films, and humidity [9,23,24].

Additionally, the application of KPFM (and by extension SKP) to electrochemical domains has introduced terminological ambiguity, particularly with regard to the term "Volta potential." In ambient (low-medium relative humidity (RH)) or thin film electrolyte environments, a clear understanding of contributions such as band bending, surface dipoles, and localized charge is essential for accurate interpretation, especially in complex material systems such as alloys with various phases [25–27], grain or morphological boundaries [28], and varying crystallographic orientations [29]; semiconductor heterostructures [30,31]; heterogeneous composites [32]; and multilayered materials [33–35]. Additionally, in organic coatings, factors including metal or oxide/organic interface, coating/electrolyte interface, coating thickness, dielectric properties, distributed dipoles, trapped charges, and space-charge regions within the coating and electrolyte must also be carefully considered, as they can influence the recorded "Volta potential" [5,8,36]. So, under dry or vacuum conditions, where no electrolyte or electric double layer (EDL) is present to sustain redox equilibrium, the signal is purely electrostatic [37] and unrelated to the electrochemical potential ($\bar{\mu}$).

Yet in the corrosion literature, CPD measured in ambient air is often referred to as "Volta potential," conflating electrostatic and electrochemical concepts [38]. Recent work has shown that surface oxidation, adsorbates, tip bias, lift height, and environmental aging can drastically shift CPD values, even inverting the apparent nobility of microstructural features [5,7]. Uhlig [39] recognized that Volta potentials measured in air can exhibit some alignment with the electrochemical series (electromotive force series), due to shared trends with work function and ionization energy. However, he emphasized that these values are highly sensitive to surface films, oxide states, and environmental exposure, making Volta potential a surface-conditioned indicator rather than a reliable or intrinsic electrochemical measurement. Extending this understanding, Birbilis et al [40] noted that, for aluminum-based alloys, the Volta potential signal can be immensely valuable for assessing the extent and morphology of damage accumulation. Nevertheless, they stressed that such measurements do not yield fundamental information regarding the intrinsic electrochemical characteristics of intermetallic particles.

Taken together, these studies demonstrate that while Volta potential mapping is an invaluable tool for visualizing heterogeneity and damage accumulation, its quantitative interpretation requires caution. As De Wit [41] emphasized in a seminal study on Al-based alloys, local Volta potential differences cannot be straightforwardly equated with corrosion activity. Instead, meaningful interpretation must be supported by complementary electrochemical measurements (e.g., scanning electrochemical microscopy (SECM)) and microstructural characterization (e.

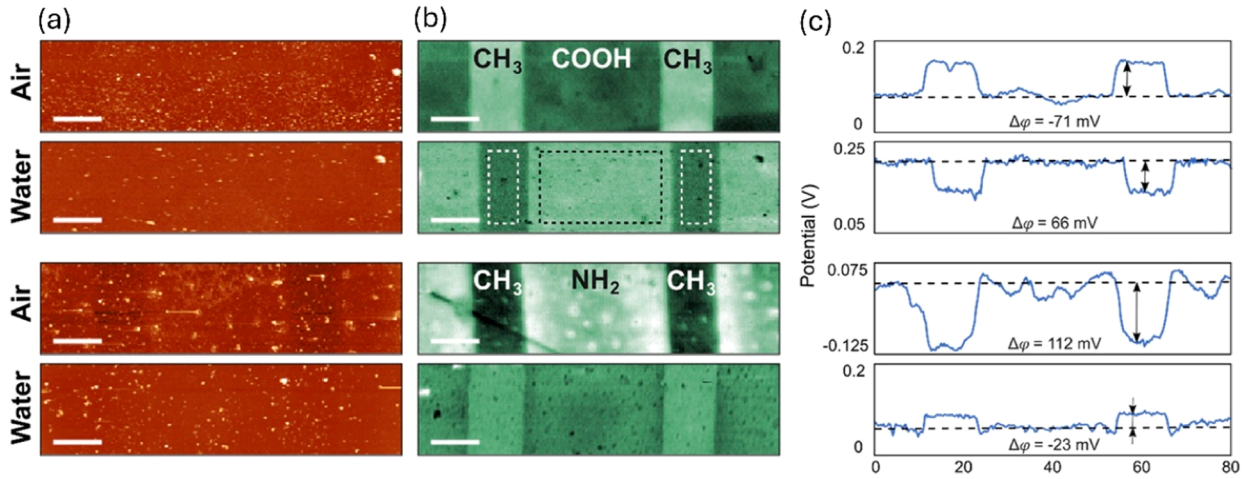

Fig. 2. (a) Topography and (b) ESPD maps acquired using AC-KPFM, with representative cross sections. (c) Measured ESPD for COOH/CH_3 and NH_2/CH_3 patterns, obtained in both air and deionized water. Adapted with permission [43] Copyright 2022, American Chemical Society.

g., scanning electron microscopy (SEM) and energy dispersive X-ray spectroscopy (EDXS)) to link Volta potential contrasts with chemical composition and corrosion morphology. Without this context, there is a risk of over-interpreting surface-conditioned Volta potential shifts as intrinsic electrochemical properties.

2. From air to electrolyte: expanding the frontiers of ESPD mapping

Emerging techniques now bridge the gap between traditional dry-environment measurements, which capture only electrostatic CPD, and in-situ liquid-phase methods, which can resolve electrochemically relevant CPD under realistic degradation conditions [42]. Two such approaches, including alternating current (AC)-KPFM and open-loop electric potential microscopy (OL-EPM), both share the key principle of applying an AC voltage between the conductive probe and the sample to modulate the electrostatic interaction while avoiding the drawbacks of low-frequency biasing in liquid (e.g., thin film or bulk electrolyte) [43,44].

In conventional or direct current (DC)-KPFM, a conductive AFM probe is scanned over the sample while an electrical bias is applied between the tip and the sample to measure the CPD. In this mode, a DC voltage is adjusted to nullify the electrostatic force between the tip and sample. In AC-KPFM, a relatively high-frequency AC modulation instead of a DC voltage is superimposed on the bias, allowing for lock-in detection of the electrostatic signal with improved sensitivity [43]. OL-EPM, while operating in an "open loop" mode without the CPD-nulling feedback, also relies on AC excitation to detect ESPD variations, making it inherently suited for liquid-phase measurements [45]. In both methods, the bias is always applied between the conductive AFM tip and the sample surface, and the resulting electrostatic force is detected through the oscillation of the AFM cantilever. Besides, optimizing the AC modulation frequency is essential to suppress Faradaic currents while maintaining stable, artifact-free mapping in liquids [42]. Fig. 1 provides a schematic overview of SKP, DC-KPFM, AC-KPFM, and OL-EPM, highlighting their operational scale, spatial resolution, and environmental compatibility. The figure illustrates the progression from macroscopic electrostatic mapping with SKP to nanoscale redox-correlated ESPD imaging with AC-KPFM and OL-EPM, capturing how each technique contributes uniquely to ESPD measurements.

In aqueous environments, however, applying a pure DC bias or any low-frequency voltage between the tip and sample can trigger unwanted electrochemical processes [42]. Polar water molecules and highly mobile electrolyte ions readily respond to the applied field (e.g., dipole reorientation, ion migration, electric double layer changes), leading to

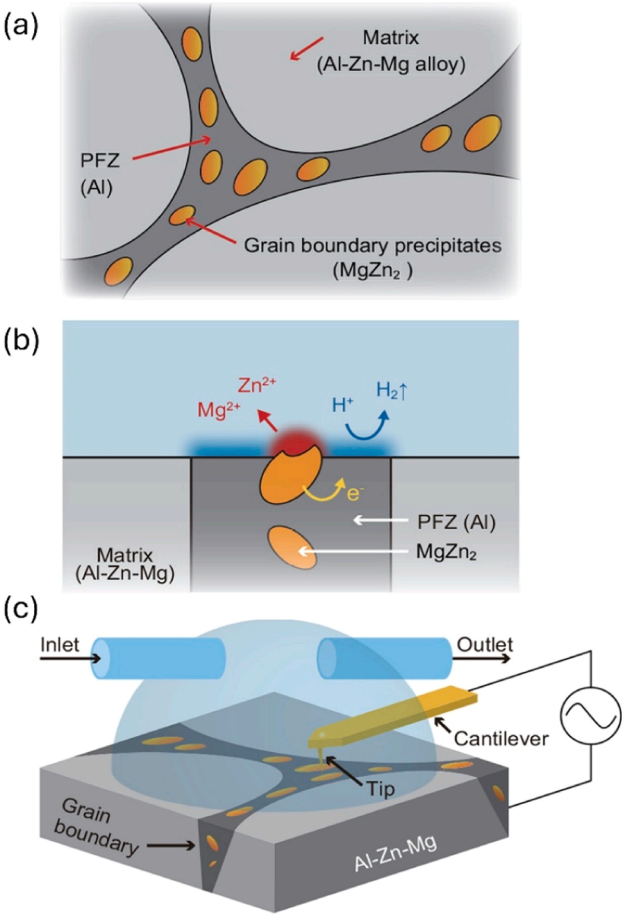

Fig. 3. (a) Model of grain boundaries (GBs) in the Al–Zn–Mg alloy. (b) Proposed GB corrosion mechanism, inferred from the corrosion potentials of Al, Al–Zn–Mg, and $MgZn_2$. (c) Experimental setup for OL-EPM measurements. Adapted with permission [47] Copyright 2023, American Chemical Society.

Faradaic reactions, electrokinetic effects, or even gas formation from electrolysis at the tip or sample surface [43]. These phenomena disrupt the measurement and compromise ESPD signal stability. Additionally, when SKP or DC-KPFM is applied to complex systems such as coating defects or delamination fronts, the detected ESPD signal is no longer a simple electrostatic signature. Instead, it becomes a convolution of

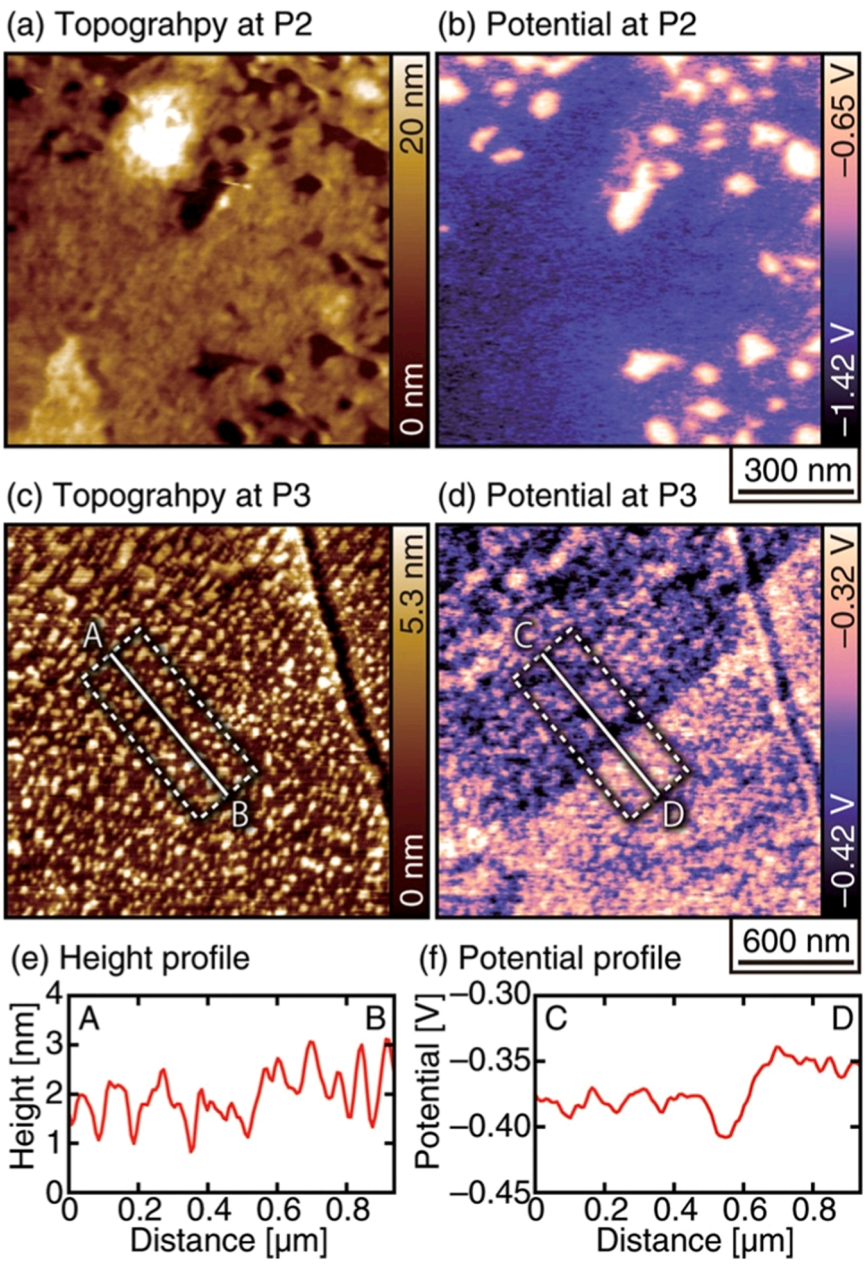

Fig. 4. Topographic and ESPD images of sensitized duplex stainless steel in an acidic solution (pH 3), recorded at locations (a, b) P2 and (c, d) P3. (a, b) Measurements in a solution containing 1 mM HCl and 1 mM NaCl. (c, d) Measurements in a solution containing 1 mM HCl only. (e, f) Corresponding height and potential profiles for images (c) and (d). Adapted with permission [45] Copyright 2016, American Chemical Society.

electrostatic differences with galvanic polarization, solution resistance, and ionic conduction within the defect volume [46]. Under these conditions, the DC nulling process can also be perturbed by parasitic voltages arising from dielectric charging of the coating, dipole layers at buried interfaces, and the superposition of multiple metal/-organic/electrolyte boundaries [8], making quantitative separation of electrostatic and electrochemical contributions inherently challenging. Therefore, both AC-KPFM and OL-EPM are particularly suitable for in-situ electrochemical studies where maintaining the native electrolyte environment is essential, with the measured signals potentially influenced by interfacial phenomena such as Stern layer formation and variations in zeta potential [43].

In a landmark study, Hackl et al [43] characterized the ESPD distribution of micropatterned self-assembled monolayers (SAMs) of CH_3/COOH and CH_3/NH_2 terminated alkanethiols on gold, both in air and in deionized water (Fig. 2). When AC-KPFM is performed in deionized water at the same sample locations as in air, a reversal in the ESPD sign is observed (Fig. 2). Topography and ESPD maps were recorded in air and deionized water, and ESPD values within the dashed rectangles were used for statistical analysis (Scale bar = 10 μm; topography color range = 100 nm; potential color range = 200 mV). In water, COOH regions appear more positive, whereas NH_2 regions appear more negative relative to CH_3 regions. This reversal can be attributed to the presence of mobile ions in solution, which form the initial countercharge layer of the EDL at the interface between water and the immobile alkanethiol SAM, namely the Stern layer [43].

Using another approach, Yamamoto et al [47]. applied OL-EPM to visualize corrosion evolutions in Al-Zn-Mg alloys, revealing pH-dependent ESPD distributions, shaped by redox potential and local corrosion cells, that differentiate anodic and cathodic regions in real time. This study provided new mechanistic insight into the corrosion behavior of $MgZn_2$ precipitates at grain boundaries in H_2SO_4 solution

(Figs. 3a and 3b). The OL-EPM measurements were conducted using the experimental setup shown in Fig. 3c, which allowed visualization of pH-dependent ESPD distributions in real time.

Similarly, Honbo et al [45] employed operando OL-EPM to map anodic and cathodic sites in situ, investigating the local visualization of corrosion behavior of sensitized duplex stainless steel (UNS S32750), particularly in weld-sensitized regions where corrosion resistance is compromised (Fig. 4). Measurements were performed with $V_{ac} = 0.8$ V, $f_1 = 700$ kHz, $f_2 = 730$ kHz. The 0 nm reference in the topographic images is arbitrary. Measurements at locations P2 (Figs. 4a and 4b) were conducted in 1 mM HCl + 1 mM NaCl, and at P3 (Figs. 4c and 4d) in 1 mM HCl only. Corresponding height and potential profiles for P3 are shown in Figs. 4e and 4f.

Eventually, both AC-KPFM and OL-EPM enable nanoscale ESPD mapping in environments where conventional DC-KPFM cannot operate stably, such as fully liquid or highly hydrated conditions. Their spatial resolution matches that of standard DC-KPFM in dry conditions, but their AC-based detection schemes allow this resolution to be retained in electrochemically relevant environments. While both AC-KPFM and OL-EPM do not directly measure the formal electrochemical potential, they enable mapping of ESPD and influenced charge variations that correlate with redox activity at the nanoscale [45].

This distinction is crucial: the formal electrochemical potential is a thermodynamic quantity defined at equilibrium, whereas the signals obtained in AC-KPFM or OL-EPM correspond to relative changes in local ESPD. These arise from interfacial charge redistribution, double-layer polarization, or redox-associated ion dynamics, and are therefore non-absolute by nature [42]. AC-KPFM achieves this by using high-frequency AC modulation that electrolyte ions cannot follow, thereby suppressing Faradaic currents and minimizing electrochemical perturbation at the interface [43]. OL-EPM adopts the same principle but operates without a feedback loop, avoiding bias-driven interference with the electrochemical environment [45]. As a result, both techniques provide electrochemically meaningful insight into nanoscale charge processes, yet their outputs should be interpreted as redox-correlated ESPD maps rather than direct measures of thermodynamic electrochemical potentials [48].

By operating in an electrolyte environment and referencing a conductive probe, the method captures local ESPD that are sensitive to surface chemistry, surface hydration, and surface charge distribution. This allows researchers to distinguish subtle variations in alloy phases, oxide layers, or corrosion states, offering valuable electrochemical insight (contrast reflects localized redox activity). Nevertheless, both AC-KPFM and OL-EPM are highly sensitive to probe material, tip–sample separation, and transient interfacial states. While this sensitivity enables the detection of nanoscale heterogeneity, it also limits direct comparison with bulk electrochemical measurements.

3. Clarifying redox interpretations

While most researchers do not explicitly state that Kelvin probe techniques measure the formal electrochemical potential ($\bar{\mu}$), it is common, particularly in the field of corrosion science, for the measured potential (often referred to as the "Volta potential") to be interpreted in terms of redox reactions. For instance, regions of higher or lower ESPD are frequently described as "cathodic" or "anodic," and shifts in ESPD are directly linked to corrosion susceptibility, galvanic interactions, or passivity breakdown [49].

For instance, a study of the corrosion behavior of as-extruded Mg–8Li–3Al (LA83) alloy used KPFM to characterize its microstructure. The AlLi particles were found to exhibit a more positive potential of 340 mV higher than the matrix, a result attributed to their cathodic nature [50]. Similarly, a study of the localized corrosion behavior of the dual-phase LZ91 Mg alloy stated that KPFM analysis revealed that the β-phase had a lower Volta potential and higher electrochemical activity. This led to the formation of a thicker, more protective surface corrosion film compared to the α-phase [49]. Furthermore, in the case of hot-dip Al–Si coatings, it is reported that both the Volta potential map and the corresponding line profile confirmed that the precipitates in the coating acted as cathodes relative to the aluminum matrix. These precipitates served as cathodic sites where the oxygen reduction reaction occurred [51].

These correlations become truly meaningful only when Kelvin probe–based measurements are conducted under conditions that allow electrolyte formation and interfacial charge transfer, such as in AC-KPFM or OL-EPM, where the EDL is present and redox processes can be resolved. Under these hydrated or in situ conditions, the recorded localized ESPD can indeed carry redox-relevant information and help identify anodic and cathodic regions in real time. For example, in AC-KPFM, high-frequency bias modulation enables stable detection of ion redistribution and charge polarization within the EDL without triggering Faradaic currents, allowing the mapping of redox-driven differences in corrosion initiation sites or grain boundary activity. Similarly, OL-EPM has been shown to visualize anodic and cathodic domains in aqueous environments by capturing ESPD shifts associated with localized ion fluxes and surface charge buildup during corrosion. In both cases, the ESPD signal is not the formal electrochemical potential, but rather a redox-correlated ESPD that tracks local variations in interfacial chemistry and charge density.

By contrast, this electrochemical interpretability disappears entirely in classical SKP and DC-KPFM under dry or vacuum conditions, where no double layer exists and the signal is purely the classical electrostatic CPD. In such cases, redox-based interpretations are scientifically unwarranted, and the term "Volta potential" should only be used in its original Kelvin sense, as the electrostatic CPD arising from work function differences between conductive surfaces. The explicit message here is simple but critical: environment defines meaning. In liquid conditions, AC-KPFM and OL-EPM enable nanoscale correlation between ESPD and electrochemical behavior, whereas in dry conditions, CPD maps are strictly electrostatic work function contrasts. Confusing these regimes risks conflating two fundamentally different physical quantities.

4. Clarifying key terminology and interpretation

"Volta potential," in its original and physically valid sense, refers to the CPD between probe and sample surface and is fully applicable to both SKP and DC-KPFM, particularly in dry or vacuum environments. However, when used to infer electrochemical tendencies (such as anodic/cathodic behavior), its interpretation becomes problematic and must be treated with caution. Accordingly, the clarified position is as follows:

- The original concept of Volta potential is purely electrostatic; it is the difference in potential just outside two materials in vacuum or air (i.e., CPD). This is the classical Volta definition [3,52], and it strictly applies in dry SKP and DC-KPFM.
- In corrosion science, researchers have historically correlated Volta potential with redox behavior when using SKP [8] or hydrated KPFM setups [38]. While this reflects how the term appears in the literature, it departs from the strict definition.

Thus, to avoid ambiguity, in this work, we explicitly distinguish the terminology:

- Volta potential is reserved for electrostatic CPD in dry SKP and DC-KPFM.
- ESPD is used for measurements performed in electrolyte-covered or highly hydrated environments (AC-KPFM and OL-EPM), as this more accurately describes the measured quantity without implying a direct electrochemical potential.

Table 1
Measurement conditions and interpretive contexts for Kelvin probe techniques.

Feature Scale	SKP Macroscopic	DC-KPFM Nanoscopic	AC-KPFM Nanoscopic	OL-EPM Nanoscopic
Probe size	150 μm to 2 mm (diameter)	2–35 nm (tip radius)	5–35 nm (tip radius)	7 plus 30 nm coated gold
Probe or tip composition	Tungsten (W), gold (Au), Platinum (Pt)	Pt-Ir, Co-Cr, Pt/Co, doped Si	Pt-Ir, Co-Cr, Pt/Co, doped Si	Au coated
Lift mode	μm to mm	0–200 nm	5–200 nm	5–200 nm
Environment	Moist surface or thin water film	Dry, ambient, or vacuum	Liquid or humidified environment	Liquid or humidified environment
Measures	CPD or work function differences	CPD or work function differences	Redox-correlated local ESPD (relative, not absolute) *	Redox-correlated local ESPD (relative, not absolute) *
Interpretation Caveats	Affected by oxide resistivity, film thickness, and RH	Cannot be treated as electrochemical, even with thin electrolyte film	Requires frequency optimization to suppress Faradaic reactions	Requires frequency optimization to suppress Faradaic reactions
Recommended Term	Apparent CPD, apparent Volta potential, apparent ESPD (under high RH)	CPD or ESPD or Work function contrast	Apparent ESPD or redox-correlated ESPD	Apparent ESPD or redox-correlated ESPD

* "Relative, not absolute" means that the measured values are referenced to the probe–sample system and experimental setup. The maps indicate ESPD between local regions under identical conditions, rather than absolute thermodynamic potentials.

5. Conclusion and outlook

As KPFM and SKP become central to characterizing electrochemical systems, we must adopt terminology that reflects physical accuracy and chemical relevance:

- Dry/vacuum conditions (purely electrostatic CPD): Use "contact potential difference (CPD)", "electrostatic surface potential difference (ESPD)", or "work function contrast" to avoid implying electrochemical activity.
- Hydrated surfaces / thin-film electrolyte (partial redox equilibrium possible in humid SKP): Use "potential map" [10] to describe the spatial distribution of measured CPD values, especially in hydrated SKP, where the reference is the probe potential.
- Fully immersed / in-situ electrolyte (redox-correlated measurements in AC-KPFM and OL-EPM): Reserve "Volta potential difference" only for cases explicitly referring to the classical electrostatic CPD between; otherwise, describe outputs as "ESPD" or "redox-correlated surface potential" depending on the context.
- AC-KPFM and OL-EPM provide unprecedented spatial resolution of redox-active behavior, but require careful experimental design, environmental control, and theoretical rigor to yield electrochemically meaningful insights

The concept of the Volta potential is rooted in electrostatics and was later adapted to describe redox-sensitive behavior in complex environments. As Kelvin probe techniques advance and enter new scientific domains, it becomes increasingly important to distinguish between the physical and electrochemical interpretations of the measured signal. With the rise of AC-KPFM and OL-EPM researchers now have tools to visualize the direct and simultaneous effect of the redox processes on the "localized ESPD" signal at the nanoscale. These methods promise to bridge physics and electrochemistry, but only if the terminology remains precise. By adopting language grounded in measurement physics and environmental context, the community can ensure that Kelvin probe data supports robust, reproducible insights across disciplines. Finally, Table 1 summarizes how the measurement environment, technique, and interfacial conditions shape the interpretation and appropriate terminology of ESPD obtained via classical SKP, DC-KPFM, AC-KPFM, and OL-EPM.

CRediT authorship contribution statement

Ehsan Rahimi: Writing – review & editing, Writing – original draft, Visualization, Validation, Investigation, Formal analysis, Data curation, Conceptualization. **Patrick Mesquida:** Writing – review & editing, Validation, Formal analysis. **Thilo Glatzel:** Writing – review & editing, Validation, Formal analysis. **Yaiza Gonzalez Garcia:** Writing – review & editing, Validation, Formal analysis. **Arjan Mol:** Writing – review & editing, Validation, Supervision, Formal analysis.

Declaration of competing interest

The authors declare that they have no known competing financial interests or personal relationships that could have appeared to influence the work reported in this paper.

Acknowledgements

The author gratefully acknowledges TU Delft for providing access to institutional resources and the availability of open-access scientific literature that enabled this contribution. T.Glatzel acknowledges financial support from the Swiss National Science Foundation (SNSF, Nanocontrol 200021L-219983, SiDoQu 200021–231373) and the Swiss Nanoscience Institute (SNI).

Data availability

Data will be made available on request.

References

[1] W. Melitz, J. Shen, A.C. Kummel, S. Lee, Kelvin probe force microscopy and its application, Surf. Sci. Rep. 66 (2011) 1–27.
[2] T. Glatzel, S. Sadewasser, M.C. Lux-Steiner, Amplitude or frequency modulation-detection in Kelvin probe force microscopy, Appl. Surf. Sci. 210 (2003) 84–89.
[3] I.F. Patai, M.A. Pomerantz, Contact potential differences, J. Frankl. Inst. 252 (1951) 239–260.
[4] K. Bian, C. Gerber, A.J. Heinrich, D.J. Müller, S. Scheuring, Y. Jiang, Scanning probe microscopy, Nat. Rev. Methods Primers. 1 (2021) 36.
[5] E. Rahimi, A. Imani, M. Lekka, F. Andreatta, Y. Gonzalez-Garcia, J.M.C. Mol, E. Asselin, L. Fedrizzi, Morphological and surface potential characterization of protein nanobiofilm formation on magnesium alloy oxide: their role in biodegradation, Langmuir 38 (2022) 10854–10866.
[6] A. Imani, E. Rahimi, M. Lekka, F. Andreatta, M. Magnan, Y. Gonzalez-Garcia, A. Mol, R.K.S. Raman, L. Fedrizzi, E. Asselin, Albumin protein impact on early-stage In vitro biodegradation of magnesium alloy (WE43), ACS. Appl. Mater. Interfaces. 16 (2024) 1659–1674.
[7] C. Örnek, C. Leygraf, J. Pan, On the Volta potential measured by KPFM–fundamental and practical aspects with relevance to corrosion science, Corros. Eng. Sci. Technol. 54 (2019) 185–198.
[8] A. Nazarov, D. Thierry, Application of scanning kelvin probe in the study of protective paints, Front. Mater. 6 (2019) 192.
[9] M. Rohwerder, F. Turcu, High-resolution Kelvin probe microscopy in corrosion science: scanning Kelvin probe force microscopy (KPFM) versus classical scanning Kelvin probe (SKP), Electrochim. Acta 53 (2007) 290–299.
[10] I.C.D. Lenton, F. Pertl, L. Shafeek, S.R. Waitukaitis, Beyond the blur: using experimentally determined point spread functions to improve scanning Kelvin probe imaging, J. Appl. Phys. (2024) 136.
[11] J.M.R. Weaver, D.W. Abraham, High resolution atomic force microscopy potentiometry, J. Vac. Sci. Technol. B 9 (1991) 1559–1561.
[12] M. Nonnenmacher, M.P. O'Boyle, H.K. Wickramasinghe, Kelvin probe force microscopy, Appl. Phys. Lett. 58 (1991) 2921–2923.

[13] S. Sadewasser, T. Glatzel, Kelvin Probe Force Microscopy, Springer, 2012.
[14] E. Rahimi, A. Imani, D. Kim, M. Rahimi, L. Fedrizzi, A. Mol, E. Asselin, S. Pané, M. Lekka, Physicochemical changes of apoferritin protein during biodegradation of magnetic metal oxide nanoparticles, ACS. Appl. Mater. Interfaces. 16 (2024) 53299–53310.
[15] E. Gachon, P. Mesquida, Mechanical properties of collagen fibrils determined by buckling analysis, Acta Biomater. 149 (2022) 60–68.
[16] B. Mallada, A. Gallardo, M. Lamanec, B. de la Torre, V. Špirko, P. Hobza, P. Jelinek, Real-space imaging of anisotropic charge of σ-hole by means of Kelvin probe force microscopy, Science 374 (2021) 863–867.
[17] M. Checa, A.S. Fuhr, C. Sun, R. Vasudevan, M. Ziatdinov, I. Ivanov, S.J. Yun, K. Xiao, A. Sehirlioglu, Y. Kim, P. Sharma, K.P. Kelley, N. Domingo, S. Jesse, L. Collins, High-speed mapping of surface charge dynamics using sparse scanning Kelvin probe force microscopy, Nat. Commun. 14 (2023) 7196.
[18] N. Khayatan, J.M. Prabhakar, E. Jalilian, N. Madelat, H. Terryn, M. Rohwerder, On the rate determining step of cathodic delamination of delamination-resistant organic coatings, Corros. Sci. 239 (2024) 112396.
[19] A. Nazarov, M.G. Olivier, D. Thierry, SKP and FT-IR microscopy study of the paint corrosion de-adhesion from the surface of galvanized steel, Prog. Org. Coat. 74 (2012) 356–364.
[20] D. de la Fuente, B. Chico, M. Morcillo, A SEM/XPS/SKP study on the distribution of chlorides in contaminated rusty steel, Corros. Sci. 48 (2006) 2304–2316.
[21] M. Stratmann, H. Streckel, On the atmospheric corrosion of metals which are covered with thin electrolyte layers—I. Verification of the experimental technique, Corros. Sci. 30 (1990) 681–696.
[22] A.P. Nazarov, D. Thierry, Scanning Kelvin probe study of metal/polymer interfaces, Electrochim. Acta 49 (2004) 2955–2964.
[23] F.N. Afshar, J.H.W. de Wit, H. Terryn, J.M.C. Mol, Scanning Kelvin probe force microscopy as a means of predicting the electrochemical characteristics of the surface of a modified AA4xxx/AA3xxx (Al alloys) brazing sheet, Electrochim. Acta 88 (2013) 330–339.
[24] F.N. Afshar, A.M. Glenn, J.H.W. de Wit, H. Terryn, J.M.C. Mol, A combined electron probe micro analysis and scanning kelvin probe force microscopy study of a modified AA4xxx/AA3xxx aluminium brazing sheet, Electrochim. Acta 104 (2013) 48–63.
[25] C. Örnek, D.L. Engelberg, KPFM measured volta potential correlated with strain localisation in microstructure to understand corrosion susceptibility of cold-rolled grade 2205 duplex stainless steel, Corros. Sci. 99 (2015) 164–171.
[26] E. Rahimi, A. Rafsanjani-Abbasi, A. Imani, A. Davoodi, TiO2/Cu2O coupled oxide films in Cl− ion containing solution: volta potential and electronic properties characterization by scanning probe microscopy, Mater. Chem. Phys. 212 (2018) 403–407.
[27] E. Rahimi, A. Rafsanjani-Abbasi, A. Imani, S. Hosseinpour, A. Davoodi, Correlation of surface volta potential with galvanic corrosion initiation sites in solid-state welded Ti-Cu bimetal using AFM-KPFM, Corros. Sci. 140 (2018) 30–39.
[28] E. Rahimi, T. Nijdam, A. Jahagirdar, E. Broitman, A. Mol, Advanced nodular thin dense chromium coating: superior corrosion resistance, ACS. Appl. Mater. Interfaces. 17 (2025) 8588–8600.
[29] A. Ma, L. Zhang, D. Engelberg, Q. Hu, S. Guan, Y. Zheng, Understanding crystallographic orientation dependent dissolution rates of 90Cu-10Ni alloy: new insights based on AFM/KPFM measurements and coordination number/electronic structure calculations, Corros. Sci. 164 (2020) 108320.
[30] M.J. Shearer, M.Y. Li, L.J. Li, S. Jin, R.J. Hamers, Nanoscale surface photovoltage mapping of 2D materials and heterostructures by illuminated Kelvin Probe force microscopy, J. Phys. Chem. C 122 (2018) 13564–13571.
[31] Y. Rosenwaks, R. Shikler, T. Glatzel, S. Sadewasser, Kelvin probe force microscopy of semiconductor surface defects, Phys. Rev. B 70 (2004) 085320.
[32] O.A. Castañeda-Uribe, R. Reifenberger, A. Raman, A. Avila, Depth-sensitive subsurface imaging of polymer nanocomposites using second harmonic Kelvin probe force microscopy, ACS. Nano 9 (2015) 2938–2947.
[33] I. Spajić, E. Rahimi, M. Lekka, R. Offoiach, L. Fedrizzi, I. Milošev, Al2O3 and HfO2 atomic layers deposited in single and multilayer configurations on titanium and on stainless steel for biomedical applications, J. Electrochem. Soc. 168 (2021) 071510.
[34] E. Rahimi, T. Nijdam, A. Jahagirdar, E. Broitman, A. Mol, A combined microstructural, electrochemical and nanomechanical study of the corrosion and passivation properties of a Cr/CrN multilayer coating, Corros. Sci. 252 (2025) 112943.
[35] E. Rahimi, R. Offoiach, S. Deng, X. Chen, S. Pané, L. Fedrizzi, M. Lekka, Corrosion mechanisms of magnetic microrobotic platforms in protein media, Appl. Mater. Today 24 (2021) 101135.
[36] E. Rahimi, R. Offoiach, M. Lekka, L. Fedrizzi, Electronic properties and surface potential evaluations at the protein nano-biofilm/oxide interface: impact on corrosion and biodegradation, Colloids Surf. B 212 (2022) 112346.
[37] S. Sadewasser, T. Glatzel, M. Rusu, A. Jäger-Waldau, M.C. Lux-Steiner, High-resolution work function imaging of single grains of semiconductor surfaces, Appl. Phys. Lett. 80 (2002) 2979–2981.
[38] Y. Liew, C. Örnek, J. Pan, D. Thierry, S. Wijesinghe, D.J. Blackwood, In-situ time-lapse KPFM investigation of sensitized AA5083 aluminum alloy to understand localized corrosion, J. Electrochem. Soc. 167 (2020) 141502.
[39] H.H. Uhlig, Volta potentials of the copper-nickel alloys and several metals in air, J. Appl. Phys. 22 (1951) 1399–1403.
[40] N. Birbilis, R.G. Buchheit, Electrochemical characteristics of intermetallic phases in aluminum alloys: an experimental survey and discussion, J. Electrochem. Soc. 152 (2005) B140.
[41] J.H.W. de Wit, Local potential measurements with the KPFM on aluminium alloys, Electrochim. Acta 49 (2004) 2841–2850.
[42] L. Collins, J.I. Kilpatrick, S.V. Kalinin, B.J. Rodriguez, Towards nanoscale electrical measurements in liquid by advanced KPFM techniques: a review, Rep. Prog. Phys. 81 (2018) 086101.
[43] T. Hackl, G. Schitter, P. Mesquida, AC Kelvin probe force microscopy enables charge mapping in water, ACS. Nano 16 (2022) 17982–17990.
[44] K. Hirata, J.i. Omi, D. Taniguchi, K. Miyazawa, F. Komatsu, Y. Takahashi, T. Fukuma, Corrosion inspection for hard disk Media with carbon-based overcoats by In-liquid open-loop electric potential microscopy, ACS. Appl. Mater. Interfaces. 16 (2024) 70020–70027.
[45] K. Honbo, S. Ogata, T. Kitagawa, T. Okamoto, N. Kobayashi, I. Sugimoto, S. Shima, A. Fukunaga, C. Takatoh, T. Fukuma, Visualizing nanoscale distribution of corrosion cells by open-loop electric potential microscopy, ACS. Nano 10 (2016) 2575–2583.
[46] N. Khayatan, M. Rohwerder, A new insight into the rate determining step of cathodic delamination, Corros. Sci. 202 (2022) 110311.
[47] S. Yamamoto, D. Taniguchi, T. Okamoto, K. Hirata, T. Ozawa, T. Fukuma, Nanoscale corrosion mechanism at grain boundaries of the Al–Zn–Mg alloy investigated by open-loop electric potential microscopy, J. Phys. Chem. C 127 (2023) 5281–5288.
[48] E. Rahimi, M. Palacios-Corella, A. Mol, S. Pané, J. Puigmartí-Luis, Kelvin probe force microscopy in bionanotechnology: current advances and future perspectives, Adv. Mater., n/a e10671.
[49] Y.H. Fu, P.W. Chu, Localized corrosion behavior and surface corrosion film microstructure of a commercial dual-phase LZ91 Mg alloy, Npj. Mater. Degrad. 9 (2025) 19.
[50] Z. Hu, Z. Yin, Z. Yin, K. Wang, Q. Liu, P. Sun, H. Yan, H. Song, C. Luo, H. Guan, C. Luc, Corrosion behavior characterization of as extruded Mg-8Li-3Al alloy with minor alloying elements (Gd, Sn and Cu) by scanning Kelvin probe force microscopy, Corros. Sci. 176 (2020) 108923.
[51] C.P. Couto, R.I. Revilla, M.A. Colosio, I. Costa, Z. Panossian, I. De Graeve, H. Terryn, J.L. Rossi, Electrochemical behaviour of 22MnB5 steel coated with hot-dip Al-Si before and after hot-stamping process investigated by means of scanning Kelvin probe microscopy, Corros. Sci. 174 (2020) 108811.
[52] L. Kelvin, V. Contact electricity of metals, Lond. Edinb. Dublin Philos. Mag. J. Sci. 46 (1898) 82–120.